Proceedings of the ASME 2020 39th International Conference on Ocean, Offshore and Arctic Engineering
OMAE2020
August 3-7, 2020, Virtual, Online

OMAE2020-18875

HYDRODYNAMIC LOADS ON NET PANELS WITH DIFFERENT SOLIDITIES

Heidi Moe Føre[1], Per Christian Endresen, Carina Norvik
EXPOSED Aquaculture Research Centre
SINTEF Ocean
Trondheim, Norway

Pål Lader
EXPOSED Aquaculture Research Centre
Norwegian University of Science and Technology (NTNU)
Trondheim, Norway

ABSTRACT

Drag forces on nets represent the largest contribution to hydrodynamic loads on traditional fish farms, and will have a large impact on total loads on new designs utilizing netting as containment method. Precise methods for estimation of drag loads are needed.

This paper gives new knowledge on hydrodynamic forces acting on aquaculture nets. It presents results from towing tests, including updated drag and lift coefficients for Raschel knitted netting materials used in nets for aquaculture, and quantify wake effect. The results include high solidity nets and high towing velocities.

It was found that drag loads were close to proportional with the netting solidity for netting solidities ranging from 0.15 to 0.32. The wake effect is quantified through the average velocity reduction factor, which is given as a linear function of solidity.

Much of previously published data are close to the data found through these tests. However, for high solidity nets, the deviation is significant. Therefore, previously published data and models may overestimate drag loads for high solidity nets.

NOMENCLATURE

A	area of netting rectangle, equal to $B \cdot H$
B	breadth of netting rectangle, inner breadth of frame
C_D	drag coefficient
C_L	lift coefficient
F_D	drag load (horizontal load component)
F_L	lift load (vertical load component)
H	height of netting rectangle, inner height of frame
ν	kinematic viscosity (10^{-6} m^2/s)
r	velocity reduction factor
ρ	water density (998 kg/m^3)
Re	Reynolds number
Sn	solidity of netting, set equal to $2 \cdot t/s$
t	twine thickness
θ	rotation angle (panel rotation about y-axis)
U	relative velocity between panel and water. Equal to towing velocity.
s	mesh side

INTRODUCTION

Several new fish farms are deployed farther from the coast than previously. This is a result of increased demand for farmed fish combined with environmental concerns, area planning conflicts and a potential for increased production. Many of these more offshore structures must withstand higher environmental loads than fish farms situated in more sheltered locations. Fish farming at more exposed sites require robust and reliable structures which facilitate safe and efficient production.

Drag forces on nets represent the largest contribution to hydrodynamic loads on traditional fish farms, and will have a large impact on total loads on new designs utilizing netting for containment of fish. Precise methods for estimation of drag loads are needed. Estimation of drag forces on nets is not straight forward due to the complexity of the local geometry of the netting, non-linear effects such as large deformations and fluid-structure interaction between the net and water flow. Experiments are needed to develop and validate theory and methods to model both forces on the netting and water flow through and around the netting.

From the late 1980s and onward several experiments have been conducted and models for hydrodynamic forces on nets used in aquaculture have been developed. Tests are usually

[1] Contact author: Heidi.moe.fore@sintef.no

performed on 2D rectangular net panels or 3D net structures with similar shape as net cages used in fish farming [1]-[8]. A common feature of established load models is that they estimate forces on a net panel, with the assumption that the contributions can be summed to represent a complete net cage. Load models are based on the netting solidity and the inclination angle between the net panel and the water flow. Netting solidity is defined as the relationship between the projected area of the netting material and the total area of the net panel [9]. It is common to decompose hydrodynamic load acting on the net panel into two components, namely drag and lift forces. Drag forces are directed parallel to the water flow, while lift forces act perpendicular to the drag force.

Based on experiments on square net panels [1], a method to calculate forces on net panels due to steady water flow was developed [2]. The experiments were performed on full scale netting with solidity ranging from 0.13 to 0.32 and tested for flow velocities of 0.16 m/s to 0.97 m/s in a towing tank. It was found that the drag forces increased greatly from a solidity of 0.24 to a solidity of 0.32. In [2] this is reflected in the established expression for drag force on a panel normal to the flow, which is given as a third degree polynomial function of the solidity. Although the netting used in [1] were of a different type than commonly used today (knotted netting instead of Raschel-knitted netting), the formulas derived by [2] are still used.

More recently published towing tests on net panels included netting of solidities from 0.06 to 0.235, towed at velocities yielding Reynolds numbers ranging from 70 to 3500 (with respect to twine diameter) [4]-[6]. In general, the resulting drag coefficients from these tests decreased with increasing Reynolds number. The rate of decrease was highest for Reynolds numbers below 500, similar to a circular cylinder [10]. The drag coefficient of the netting twines did not reach that of a similar circular cylinder for high Reynolds numbers, probably due to hydrodynamic interaction between the twines [6]. However, this was also true for the lowest solidity tested (0.128) where the interaction is expected to be low. Data presented in [3], [4] and [6] indicate that the drag coefficient for net panels is dependent on Reynolds number, but is relatively constant for Reynolds numbers between 1500 and 3500.

The main factor in determining the drag coefficient is netting solidity. Solidity is well defined, but the method for determining solidity varies: Twine diameter and mesh bar length has been used to estimate the solidity under the assumption that the net consists of crossing twines with no added area in the joints (mesh corners) [4], and the increase in area due to twine intersections has also been accounted for [6]. Others use image analysis to determine solidity directly [5]. These different methods will yield different solidity values. At present there does not exist a uniform standard regarding measurement of netting dimensions and determination of netting solidity [11]. In addition, solidity is not a constant feature, but will change over the lifetime of the net (e.g. shrinking of netting).

This paper gives new knowledge on hydrodynamic forces acting on aquaculture nets. It presents results from towing tests, including updated drag and lift coefficients for Raschel knitted netting materials used in nets for aquaculture. The results include a high solidity net (0.32) and high towing velocities. Panels with netting of varying solidity and inclination angle were towed at different velocities while loads acting on the panels and relative velocities in the water behind the panels were measured. Resulting loads, load coefficients and wake effects are presented.

MATERIALS AND METHODS

Netting materials

Four different netting materials were used in these tests as described by mesh size, twine thickness and solidity in Table 1. All netting materials were traditional Raschel knitted PA6 multifilament netting, the so-called knotless netting. The lowest solidity nets (N15, N16 and N23) are commercial netting, i.e. with full scale dimensions. N32 is Raschel knitted netting with smaller meshes, typically applied in landing nets, and will in this context represent a scaled net with high solidity. The scaling factor of N32 is 2-4 for typical full-scale net dimensions used in net cages for salmon culture.

Establishing objective measures of mesh side, twine thickness and solidity is not trivial. Raschel knitted netting is soft and flexible, and netting dimensions will change for low loads. In practice, mesh side and solidity will depend on tensile loading, or stretching of the netting. The twine thickness will vary along the twine, and the twine may be compressed during thickness measurements.

Dimensions in Table 1 were measured on dry unloaded netting using a ruler and a slide caliper. The netting was placed on a plane surface and stretched with light hand force to form square meshes. The length over ten meshes was measured, and mesh side (s) was found as this number divided by ten. Twine thickness (t) was found using a slide caliper with blunt edges, which was tightened over the twine without compressing the twine (the caliper could be moved along the twine length). Based on these measurements, the solidity of the net was estimated as

$$Sn = 2 \cdot t/s \tag{1}$$

Set-up

A rectangular piece of netting with square meshes was attached to a rectangular steel frame made of circular steel tubes with an outer diameter of 16 mm, forming a net panel. In addition, two thin steel wires were attached along the diagonals to form a supporting cross behind the netting in order to limit deformation of the netting during towing. The netting was mounted so that the "right" side of the netting, i.e. the side with V-shaped stiches, was facing the towing direction [11]. The inner dimensions of the square had a breadth of $B = 1215$ mm and a height of $H = 985$ mm.

When the netting was mounted in the panel, the mesh side was larger than the nominal dry values in Table 1 as shown in Table 2. This is mainly due to wetting of the netting. When the

netting is wetted, the dimensions will in general increase up to 10% because polyamide will absorb water [12]. To limit deformations of the netting during towing, the netting was first wetted and then mounted to the frame. In addition, slight hand force was used to mount the netting tightly to the frame. Therefore, during towing the mesh side of the netting was 10-12% larger for N15, N16 and N23, and 4 % larger for N32, compared to unloaded, dry netting. The solidity of the netting mounted in the panels was reduced compared to dry unloaded netting.

The frame surrounding the netting was attached to four 3 DOF load sensors, placed on the aft side of the net, two over the panel height at each side (Figure 1). One of these two sensors was clamped, while the other was free to move along the steel tube of the frame to prevent axial loads in the frame between these grips. At the other end the load sensors were attached to the main rig. These connection points were hinged in different DOFs to avoid internal strain in the test frame. The rig itself was given a streamlined shape with a foil shaped cross section to minimize the impact from the rig on the flow through the panel.

Towing tests were performed in one of SINTEF Ocean's towing tanks in Trondheim, Norway, known as the ship model tank. This tank is 10.5 m wide and 5.6 m deep, and a length of 175 m was applied in these tests. The towing carriage, mounted across the tank width, was run at velocities ranging from 0.25 – 2.0 m/s in negative x-direction, representing relevant velocities for estimation of drag loads on cages for fish farming.

In vertical position ($\theta = 0°$), the top of the net panel was 39 cm below the water surface, while for a rotation angle of $\theta = 67.5°$ about the y-axis the distance was 26 cm. The rotation angle is found between the panel normal vector and the towing direction.

Relative velocity was measured after the vertical panels at a horizontal distance of 71.5 cm, approximately 90 cm below the water surface (at panel center), using an acoustic doppler current meter.

17 different configurations involving different net panels, frames (panels with netting cut out) and rotation angles were towed as shown in Table 3. Towing velocities were increased from 0.25 m/s at 0.25 m/s or 0.5 m/s intervals up to the maximum velocity (Table 3). Panel N32 was towed with a maximum velocity of 1.75 m/s due to the relatively high loads and the limitations of the load sensors. All four net panels were towed with a rotation angle of 0° and 45°, and N16 and N23 were in addition towed with a rotation of 22.5° and 67.5°. After towing of net panel N16 and N23, the netting was cut out of the panels, leaving adjacent netting sewed to the frame. Loads acting on these frames only, including grips and residual netting, cable ties and seams, were measured for all angles of net panel N23 (Table 3) and in vertical position (90°) for N16.

Table 1: Netting dimensions measured on dry unloaded netting.

Netting	Mesh side [mm]	Twine thickness [mm]	Solidity [-]
N15	29	2.7	0.17
N16	25	2.5	0.17
N23	15.5	2.0	0.25
N32	7.7	1.3	0.33

Table 2: Netting dimensions measured on wet net panel.

Netting	Mesh side [mm]	Twine thickness [mm]	Solidity [-]
N15	32.4	2.5	0.15
N16	27.5	2.2	0.16
N23	17.3	2.0	0.23
N32	8.0	1.3	0.32

Table 3: Overview of performed tests.

Netting	Max. vel. [m/s]	Rotation angle with net [°]				Rotation angle without net [°]			
		0	22.5	45	67.5	0	22.5	45	67.5
N15	2.00	X		X					
N16	2.00	X	X	X	X	X			
N23	2.00	X	X	X	X	X	X	X	X
N32	1.75	X		X					

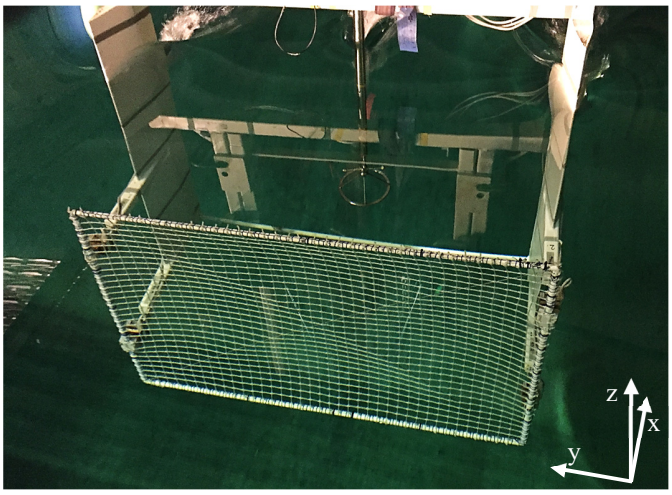

Figure 1: Test set-up (N15 at $v = 2$ m/s).

Methods for processing results

Measured loads include load contributions from the netting, the supportive frame with seams, and grips attaching the frame to the load sensors and test rig (Figure 1). It is the loads acting on the netting that are of interest and are published in the Results section. They were found by subtracting loads acting on the frame (with grips, seams and net residues) from total loads measured on the panels. After towing of panel N16 and N23, the netting was cut out of the panels along the inner perimeter of the steel rod frame, leaving net residues and seams attached to the frame. Loads acting on the frame were then measured for all rotation angles of net panel N23 (Table 3) and in vertical position (0°) for N16, for towing velocities up to 2 m/s. These measurements were then applied to estimate loads acting on the frame for the remaining tests (Table 3): For panel N16, drag loads on rotated frames were estimated as 1.22 times measured values for N23. The factor of 1.22 represents the difference in loads measured for vertical frames N16 and N23 (see Discussion chapter). Drag loads on the frame of N15 was assumed equal to N16 and loads on N32 were assumed equal to N23, based on similar mesh size of the netting.

The signals from load and velocity sensors were low-pass filtered. Presented values were averaged over a period of approximately 30 seconds during a period of stable response after accelerating the panel.

Drag and lift coefficients were calculated using Eq. 2 and components of the measured loads in horizontal (x) and vertical (z) direction.

$$C_{D,L} = \frac{2 \cdot F_{D,L}}{\rho \cdot A \cdot U^2} \tag{2}$$

where $C_{D,L}$ is the drag or lift coefficient, $F_{D,L}$ is the corresponding component of the measured load, ρ is the water density (998 kg/m^3), A is the net panel area ($B \cdot H$) and U is the relative velocity between panel and water (towing velocity).

Results are also presented as drag and lift coefficients divided by the netting solidity ($C_{D,L}/Sn$), and as a function of Reynolds number as given in Eq 3:

$$Re = \frac{U \cdot t}{\nu} = U \cdot t \cdot 10^6 \; s/m^2 \tag{3}$$

where ν is the kinematic viscosity (10^{-6} m^2/s at 20°C).

Results are also presented as $C_{D,L}/Sn$. Considering the projected area of the netting, rather than the panel area in Eq 2 (replace A with $A \cdot Sn$), the drag term of Morison's equation is the result. $C_{D,L}/Sn$ can be used as drag coefficient applying Morison's equation in load calculations on netting twines.

Relative velocity measurements behind the panels were applied to estimate how much the netting affected the water flow (wake effects): The velocity reduction factor was calculated as velocity measured after a panel with netting (U_{an}) divided by the velocity after the frame only (U_{af}) as given in Eq. 4.

$$r = \frac{U_{an}}{U_{af}} \tag{4}$$

RESULTS

Drag and lift loads

Drag loads on netting in vertical net panels and lift loads for a rotation of 45° are given in Figure 2 and 3. In addition, loads at different rotation angles are given for a velocity of 1 m/s in Figure 4.

It was found that drag loads increased close to proportional with velocity squared. Except for the highest velocities (1.75-2.0 m/s), where loads were lower. This may be due to changed flow patterns with increasing velocity, possibly causing more water to flow around the panel reducing the local inflow velocity. Loads may also be affected by deformations of the netting as a result of the hydrodynamic loads (Figure 1). Further, drag loads were close to proportional with the netting solidity.

Also lift loads increased close to proportional with velocity squared at an inclination angle of 45°, except at high velocities (Figure 3). As expected, lift increased with increased solidity, except for N15 which yielded about 20% larger lift loads than N16. This is possibly caused by errors in measurements, errors in estimating the load contribution of the frame, and/or possibly other uncertainties (see Discussion chapter). Assuming F_L to be proportional to solidity, it is possible that resulting lift loads on netting N15 are more correct than lift on N16, however no firm conclusions can be made.

Figure 4 shows development of drag and lift for different rotation angles. A towing velocity of 1 m/s was chosen as an example, as this is a common design value at typical Norwegian aquaculture sites with relatively strong water currents. The trends are similar for other towing velocities. As expected, drag loads were reduced with increased rotation, while maximum lift load values occurred around 45°.

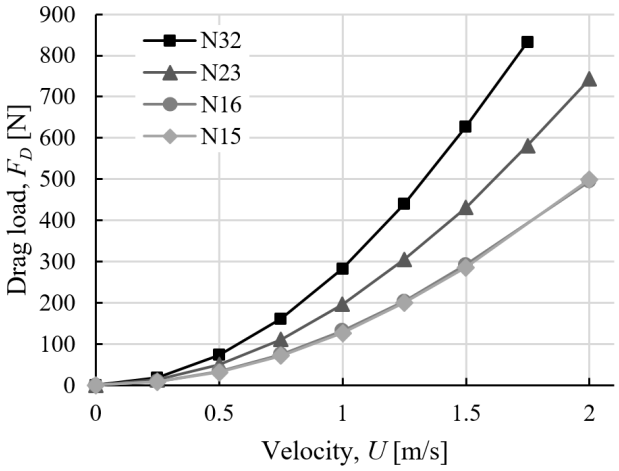

Figure 2: Drag loads on netting in vertical net panels.

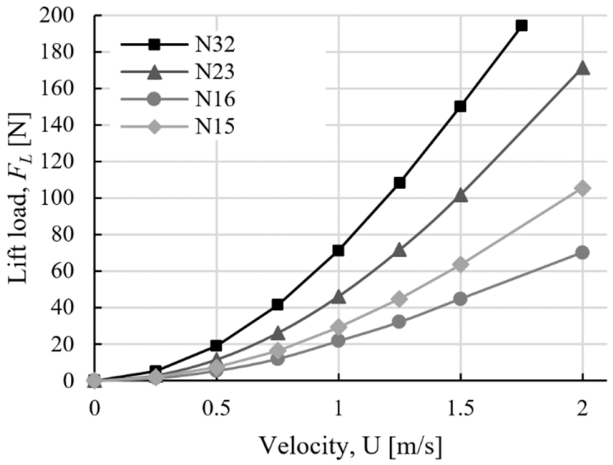

Figure 3: Lift loads on netting in panels rotated 45°.

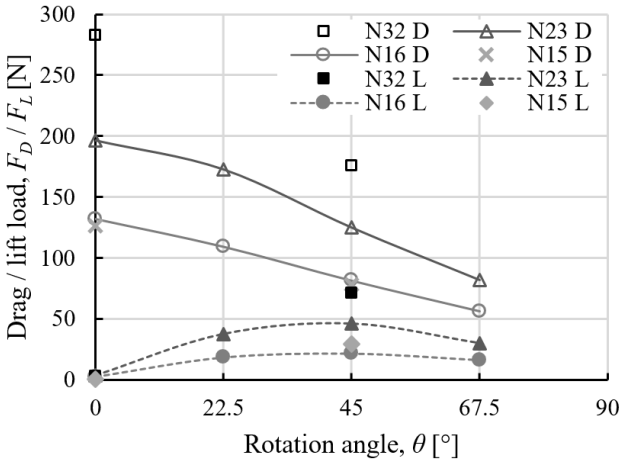

Figure 4: Drag and lift loads on netting as a function of rotation angle. Given for a towing velocity of 1.0 m/s.

Drag and lift coefficients

Drag and lift load coefficients (C_D and C_L) were calculated for the tested netting by application of Equation 2. C_D and C_L as a function of Reynolds number (*Re*) are given for vertical panels and a rotation angle of 45° respectively in Figure 5 and 6. 3rd order polynomial trend lines are indicated for each panel. Netting N32 show decreasing load coefficients with increasing *Re*, while the other three netting panels have close to constant load coefficients with a tendency to increase and decrease for the lowest and highest *Re,* respectively. This tendency is supported by Balash et al. [3], which show a distinct increase in drag coefficient for netting for $Re < 500$, and comply with trends for drag coefficients of smooth cylinders [10].

Figure 7 and 8 give drag and lift coefficients divided by the solidity, C_D/Sn, which can be applied as drag coefficient in Morison's equation to calculate drag on netting twines. For drag, this normalization assembles the data points, indicating that drag loads are close to proportional to the netting solidity for the tested solidity range (0.15 – 0.32). For rotation angles 22.5° and 45°, the two highest solidity nets (N23 and N32) show slightly higher C_D/Sn-values than the lower solidity nets (N15 and N16): For $Re \in (1000, 4000)$ and $\theta = 45°$, average C_D/Sn is 0.92 for N23 and N32 and 0.87 for N15 and N16. Similarly, for $Re \in (1000, 4000)$ and $\theta = 22.5°$, C_D/Sn is on average 1.27 and 1.19 for N23 and N16 respectively. These differences in C_D/Sn between netting panels are 6-7%, which may be within the error margins (see Discussion).

For $Re > 1000$, the resulting C_D/Sn-values show a linear, slightly downward trend for increasing *Re*. For lower *Re*, C_D/Sn tend to decrease to a higher degree with increasing Re. For $Re \in (1000, 5000)$, average values for C_D/Sn can be expressed as a first order polynomial as given in Eq. 5 using the constants given in Table 4. It was found that C_D is proportional to *Sn* and dependent on *Re* to a limited degree.

$$\frac{C_D}{Sn} = a + b \cdot Re \tag{5}$$

Lift coefficient divided by the solidity (C_L/Sn) as a function of *Re* (Figure 8) does not yield as clear trends as for drag (Figure 7). For $\theta = 45°$, the high solidity N32 yield the highest C_L/Sn-values, while N16 yield the lowest values for all angles. As mentioned previously and discussed in the Discussion chapter, it is possible that lift loads on N16 is affected by errors or uncertainties. Possible linear trend lines for C_L/Sn (1st order polynomials) are indicated. Values for N16 are neglected in these.

Table 4: Constants for 1st order polynomials describing average C_D/Sn as a function of $Re \in (1000, 5000)$ and different inclination angels, θ.

θ	a	b
0°	1.478	$-2 \cdot 10^{-5}$
22.5°	1.275	$-2 \cdot 10^{-5}$
45°	1.905	$-6 \cdot 10^{-6}$
67.5°	0.592	$4 \cdot 10^{-6}$

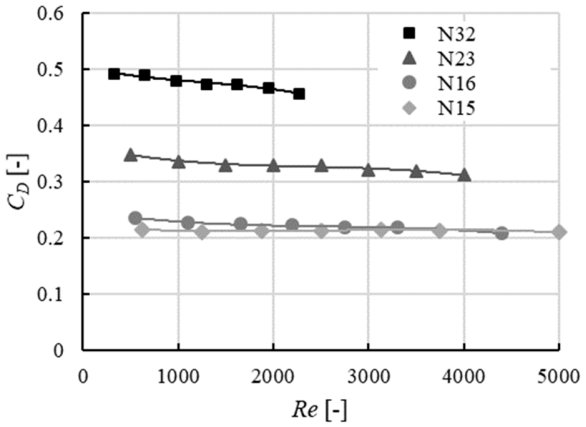

Figure 5: Drag coefficients as a function of Reynold number for the different netting dimensions in vertical position (θ = 0°).

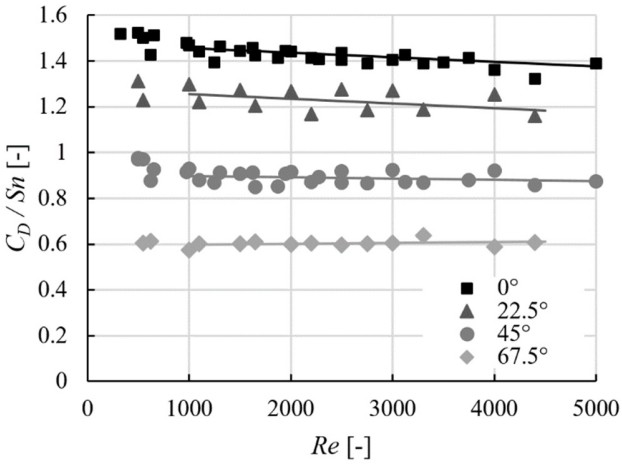

Figure 7: Drag coefficient divided by solidity for vertical (0°) and rotated panels as a function of Reynolds number.

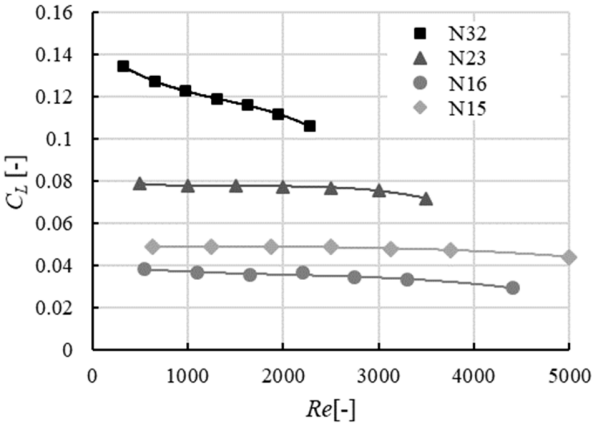

Figure 6: Lift coefficients as a function of Reynold number for the different netting dimensions with a rotation angle θ = 45°.

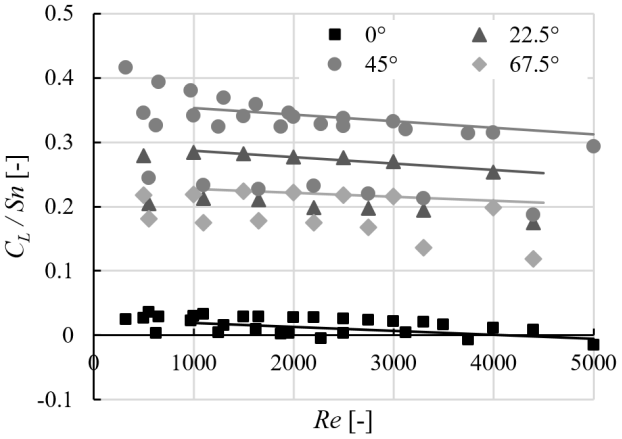

Figure 8: Lift coefficient divided by solidity for vertical (0°) and rotated panels as a function of Reynolds number.

Velocity reduction

Figure 8 gives the velocity reduction factor (r) for all vertical netting panels and towing velocities. r increases with increasing solidity and the results do not show any dependency on towing velocity. One exception is the high solidity N32, where r at the highest towing velocity of 1.75 m/s is lower than at lower velocities, which may be due to changed flow pattern (see section on drag and lift loads). On average over the velocity range of 0.5-1.5 m/s, r is 0.90, 0.88, 0.83 and 0.75 for N15, N16, N23 and N32 respectively.

Considering all data points for velocities in the range 0.5-1.5 m/s, the average velocity reduction factor may be expressed as given in Eq 6. Eq 6 is given as the stapled line in Figure 9 together with r-values for 0.5, 1.0 and 1.5 m/s for the four different panels.

$$r = 1.02 - 0.84\,Sn \tag{6}$$

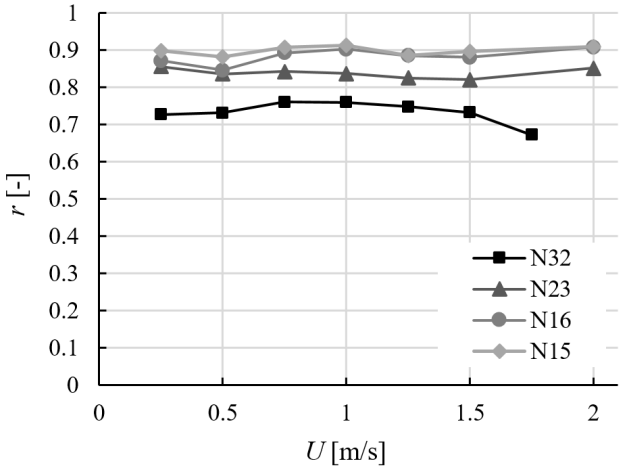

Figure 8: Velocity reduction factor as a function of towing velocity, given for different netting dimensions.

DISCUSSION

Comparison with previously published data and theory

The obtained drag loads on netting were compared to previously published results from towing tests of netting by Balash et al. [3], Zhan et al.[6], Paturson et al. [4] and Rudi et al. [1]. Established drag loads on netting as a function of netting solidity are compared for these five different experiments in Figure 10. A towing velocity of approximately 1 m/s was chosen for comparison. The results from the experiments presented in this paper provides a linear relation between the drag coefficient and the solidity, i.e. C_D is proportional to Sn. This is in accordance with theory, i.e. Morison's equation, considering the netting to be built up by cylinders with a drag coefficient of $C_{D,I}/Sn$ and neglecting possible non-linear effects for instance due to deformation of the panels. Most of the previously published data are close to the data found through the tests published in this paper. However, for high solidity nets, the deviation is significant. Previously published data and models may overestimate drag loads for high solidity nets. One explanation for this can be that the estimated solidity of the netting may be inaccurate. Rudi et al. [1] used knotted netting, which may also contribute to this deviation.

$C_{D,I}/Sn$ can be used as drag coefficient applying Morison's equation in load calculations on netting twines. Comparing these values to the established drag coefficient for smooth circular cylinders [10], it is found that the drag coefficient on net twines are approximately 40% higher than for a smooth circular cylinder. This is probably mainly due to the knots/joint in the netting and possibly increased roughness.

It was found that the loads acting on the frame was affected by the seams, net residues and the grips attaching the frame to the load sensors: Comparing measured drag loads on a vertical frame with comparative calculated loads based on Morisons equation, showed an increase of 50% for N23 and 77% for N16 at a velocity of 1 m/s.

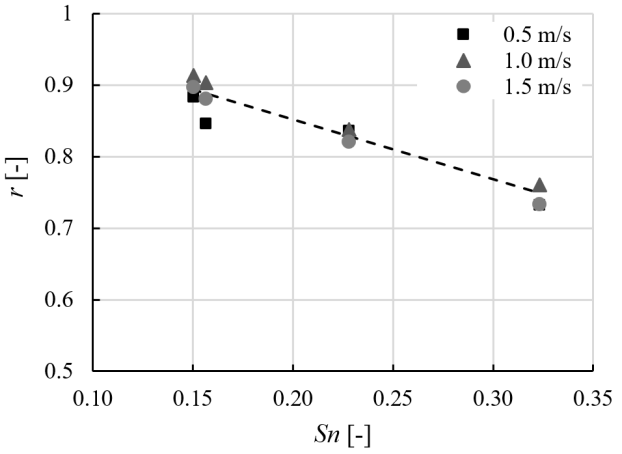

Figure 9: Velocity reduction factor for different towing velocities and solidities. Stapled line indicates a linear trend line expressed in Eq. 6.

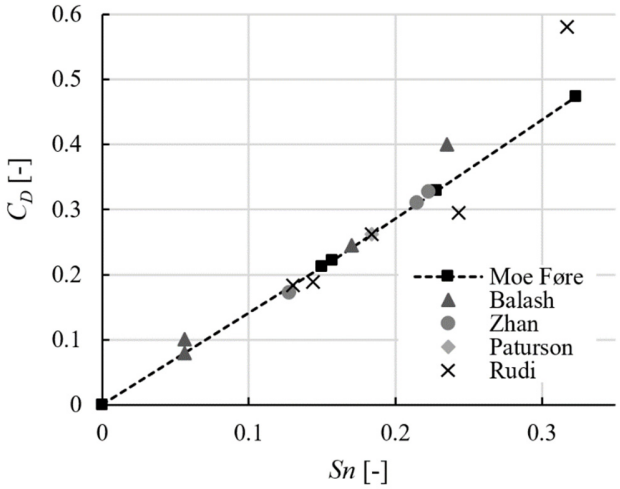

Figure 10: Drag coefficient for vertical panels towed at 1 m/s (Paturson at 0.75 m/s). Comparing data from different published towing tests with current results (Moe Føre).

Sources of error

In general, the results from the presented towing test show high accuracy; for instance, drag loads increase proportional to velocity squared as expected, except at high velocities. The magnitude of the towing velocity was given with high accuracy, which has been validated several times over the years. During the presented experiments velocity measurements in an undisturbed area at the side of the test rig confirmed the towing velocity.

However, several uncertainties must be considered when assessing the results, which is a fact for all experiments. In the presented results, this includes model imperfections, estimation of loads on supportive structures (frame and grips) and uncertainties in flow velocity measurements. Although the test rig has been carefully produced to limit imperfections, imperfections will always be present in a physical model. Small imperfections in measures and angles may affect loads acting on the net panels.

The frame encloses and supports the netting to ensure that it keeps it's rectangular and 2D shape. The frame is slender, with a diameter of 16 mm. Still, the loads acting on the frame (with grips, seams and net residues) represent a significant fraction of the total loads acting on the panel. Maximum drag loads on frame of N23 and N16 (with the netting cut out) were measured for vertical panels at U = 2 m/s as 246 N and 308 N respectively. The loads represented up to 39% of the measured drag loads on panel with netting (found for net panel N16). Similarly, for maximum measured lift loads at an angle of 45°, lift loads on the frame only were measured as 61 N for N23 and estimated as 72 N for N15 and N16. The frame represented 41% and 51% of lift loads measured on panel N15 and N16 respectively.

Panel N15 and N16 have very similar netting solidities and measured drag loads. However, lift loads found for panel N16 were lower than lift on N15: For a velocity of 2.0 m/s and a rotation angle of 45° the lift load acting on the netting was estimated to be 105 N and 70 N for N15 and N16. This may possibly be due to errors in measurements of lift loads on N16, as one would expect a similar difference in drag between the two panels at this angle, which is not observed.

The two frames that were tested with the netting cut out (Table 3), yielded different load measurements. On average, frame N16 without netting experienced 22% higher drag loads in vertical position (0°) than frame N23. This was probably due to different effect of the residual netting that was sewn to the frame. For N16, the netting did in practice increase the projected diameter of the frame, as a netting twine added to the diameter along the outer perimeter of the frame This gave a difference in estimated lift loads up to 12 N and measured drag up to 62 N between the frame of N16 and N23. Thus, a difference in maximum estimated drag and lift loads of 62 N and 10 N is probably within the margin of error for several of the tests where the loads on the frame was estimated and not measured directly. In practice, this means that the observed variations in C_D/Sn-values for netting in Figure 7 is within the margin of error, but the variations may also partly reflect physical differences in the netting materials. N15 and N16 were assumed to have the same load contribution from the frame, but this was only measured for N16 and loads for rotated frames were estimated based on measurements on the frame of N23. C_D-values for low solidity nets are relatively more affected by errors in frame load estimates, as these will represent a larger fraction of the total loads.

CONCLUSION

It was found that drag loads were close to proportional with the netting solidity for netting solidities ranging from 0.15 to 0.32. As expected, also lift increased with increased solidity, except for the lowest solidity net (N15) which yielded about 20% larger lift loads than the similar solidity N16. Lift load estimated for N15 were possibly affected by errors.

It was found that C_D is proportional to Sn and dependent on Re to a limited degree. For $Re > 1000$, the resulting drag coefficients divided by solidity show a linear, slightly downward trend for increasing Re. For lower Re, C_D/Sn tend to decrease to a higher degree with increasing Re. For $Re \in (1000, 5000)$, average values for C_D/Sn was given as first order polynomials.

Lift coefficients divided by the solidity (C_L/Sn) as a function of Re did not yield as clear trends as for drag. Possible trend lines for C_L/Sn are indicated.

The wake effect is quantified through the average velocity reduction factor, which is given as a linear function of solidity.

Much of the previously published data are close to the data found through these tests. However, for high solidity nets, the deviation is significant. Therefore, previously published data and models may overestimate drag loads for high solidity nets.

ACKNOWLEDGEMENTS

This research has been funded by the Research Council Norway, EXPOSED Aquaculture Research Centre, grant number 237790. Many thanks to the team at the SINTEF Ocean towing tank for highly skilled work and advice, and the partners of EXPOSED for the good cooperation.

REFERENCES

[1] Rudi, H., Løland, G. and Furunes, I. "Modellforsøk med nøter. Krefter og gjennomstrømning på enkeltpaneler og merdsystemer.″ SINTEF Report, Trondheim, Norway. 1989.

[2] Løland, G. "Current forces on and flow through fish farms," PhD thesis, Norwegian Institute of Technology, Division of Marine Hydrodynamics, Trondheim. 1991.

[3] Balash, Cheslav, Colbourne, Bruce, Bose, Neil, Raman-Nair, Wayne. "Aquaculture Net Drag Force and added Mass", *Aquacultural Engineering*, Volume 41, Issue 1, Pages 14-21. 2009. ISSN 0144-8609. https://doi.org/10.1016/j.aquaeng.2009.04.003.

[4] Patursson, Øystein, Swift, M. Robinson, Tsukrov, Igor, Simonsen, Knud, Baldwin, Kenneth, Fredriksson, David W., Celikkol, Barbaros. "Development of a porous media model with application to flow through and around a net panel." *Ocean Engineering*, Volume 37, Issues 2–3, Pages 314-324. 2010. ISSN 0029-8018. https://doi.org/10.1016/j.oceaneng.2009.10.001

[5] Gansel, L. C., Jensen, Ø., Lien, E., and Endresen, P. C.. "Forces on Nets With Bending Stiffness—An Experimental Study on the Effects of Flow Speed and Angle of Attack." *ASME. J. Offshore Mech. Arct. Eng*. November 2014; 136(4): 041201. https://doi.org/10.1115/1.4027954.

[6] Zhan, J.M., Jia, X.P., Li, Y.S., Sun, M.G., Guo, G.X., Hu, Y.Z. "Analytical and experimental investigation of drag on nets of fish cages.", *Aquacultural Engineering*, Volume 35, Issue 1, Pages 91-101. 2006. ISSN 144-8609. https://doi.org/10.1016/j.aquaeng.2005.08.013.

[7] Lader, P.F., Enerhaug, B. "Experimental investigation of forces and geometry of a net cage in uniform flow." *IEEE J. Oceanic Eng.* 30, 79–84. 2005.

[8] Moe-Føre, H., Lader, P.F., Lien, E. Hopperstad, O.S. Structural response of high solidity net cage models in uniform flow. Journal of Fluids and Structures 65, 180-195. 2016.

[9] NS 9415.E:2009 "Marine fish farms - Requirements for site survey, risk analyses, design, dimensioning, production, installation and operation." Standards Norway. 2009.

[10] Schlichting, H. *Bounary-Layer Theory.* McGraw-Hill Book Company, New York (1979).

[11] Moe Føre, H. and Gaarder, R. H. "RobustNot - Dokumentasjon av mekaniske egenskaper og dimensjoner til notlin i oppdrettsnøter". SINTEF Ocean. SINTEF Ocean report 2018:00971. 2018.

[12] Moe, H., Olsen, A., Hopperstad, O. S., Jensen, Ø., Fredheim, A. "Tensile properties for netting materials used in aquaculture net cages." *Aquacultural Engineering* **37**, 252–265. 2007.

[13] Lader, P., Enerhaug, B., Fredheim, A., Klebert, P. and Pettersen, B. "Forces on a cruciform/sphere structure in uniform current." *Ocean Engineering* 82: 180-190. 2014.